Design of bridges against ship collisions

Pedersen, Preben Terndrup; Chen, Jun; Zhu, Ling

Published in:
Marine Structures

Link to article, DOI:
10.1016/j.marstruc.2020.102810

Publication date:
2020

Document Version
Peer reviewed version

DESIGN OF BRIDGES AGAINST SHIP COLLISIONS

Preben Terndrup Pedersen[*] [1,2], *Jun Chen* [2,3] *Ling Zhu* [3,4]

1. Department of Mechanical Engineering, Technical University of Denmark, Lyngby, Denmark
2. Departments of Naval Architecture, Ocean and Structural Engineering, School of Transportation, Wuhan University of Technology, Wuhan, P.R. China
3. Key Laboratory of High Performance Ship Technology of Ministry of Education, School of Transportation, Wuhan University of Technology, P.R. China
4. Collaborative Innovation Centre for Advanced Ship and Deep-sea Exploration, Wuhan, China

ABSTRACT

The paper outlines a rational design procedure for bridge piers and pylons against ship collision impacts. Firstly, a set of risk acceptance criteria are proposed. This is followed by a mathematically based procedure for calculation of the probability of critical ship meeting situations near the bridge, and the probability of ship collision accidents caused by human errors as well as technical errors. This first part of the paper leads to identification of the largest striking ship, "design vessels", a given bridge pier must withstand without structural failure in order for the bridge connection to fulfil the risk acceptance criteria. The final part of the paper is devoted to an analysis of the needed impact capacity for the bridge pylons and piers exposed to ship bow impact loads from these "design vessels". For a number of different ship types and different tonnage merchant vessels, load – displacement relations for ship bow collisions against rigid walls are derived. Based on these comprehensive numerical results, a new empirical relation is derived which is suited for design against bow collisions. This expression for maximum bow collision forces is compared with a previously published expression for ice- strengthened ships and with existing standards for assessment of bow crushing forces. It is shown that there is need for an update of these existing standards. For design of piers and pylons against local impact pressure loads, a pressure - area relation for bulbous bow impacts is derived.

KEYWORDS
Ship collisions, Bridges, Design vessels, Eurocode, AASHTO, Acceptance criteria.

*Corresponding author:
E-mail Address: ptp@mek.dtu.dk

1.INTRODUCTION

Spectacular bridges are being built or are planned built over waterways with substantial ship traffic. Recent examples are the new concepts for floating bridges over very wide and deep fjords in Norway (Moan & Eidem [1]), the world's longest span suspension bridge: the Canakkale 1915 Bridge in Turkey, and the

world's longest bridge: the Hong Kong – Zhuhai – Macau Bridge. For such bridges, an important accidental load, is ship collisions. Many accidents have occurred where ships have collided against bridge piers and bridge girders such that the bridges collapsed and people travelling on the bridge killed. In addition, ship – bridge collisions often lead to disruption of the traffic on the bridge for extended periods of time. Such traffic disruptions can have severe economic consequences for the society.

The building of a bridge crossing a major waterway may also influence the ship traffic pattern by concentrating the traffic in new shipping lanes and introducing new navigational obstacles, the result being that the navigational conditions can become more difficult and lead to a higher probability of ship-ship collisions and ship grounding accidents in the vicinity. Therefore, an important design criterion for the bridge should be that the navigational span of the bridge is so large that ship collisions occur only because of navigational errors or technical failures on board of the passing vessels, and not because of increased navigational difficulties, see Ref. [2].

The main purpose of operational risk analyses is to ensure that large accidents with fatalities and lengthy interruptions are low enough to be acceptable to users, the public and the relevant authorities, but which at the same time allow an economic construction and operation of the bridge. The first part of the paper presents a discussion of such risk acceptance criteria.

It is not possible to predict or extrapolate the likelihood of future rare events such as ship collisions from similar events elsewhere. The best we can do is to use risk evaluation models even if these are difficult to verify. That is, we cannot measure or estimate the risk particularly well. However, we can decide what the level of risk should be, i.e. establish a set of acceptance criteria and then agree on what risk model we will use to verify that the selected criteria are met.

The objective of the present paper is to present such a risk model for estimation of the operational risk associated with ship collisions for bridges over navigational channels and to give guidance to bridge design.

After a presentation of some relevant risk acceptance criteria, a probabilistic procedure is outlined for calculation of "design vessels" for pylons and piers such that the specified risk acceptance criteria are met. A "design vessel" for a specific bridge structural element is defined as a striking vessel which the structural element must withstand without structural failure in order for the bridge connection to fulfil the risk acceptance criteria.

To facilitate the structural design of piers and pylons against bow impact from "design vessels", the last part of the paper is devoted to an analysis of the needed impact capacity for the bridge pylons and piers subjected to ship bow impact loads. For six different types and different tonnage merchant vessels load – displacement relations for ship bow collisions against rigid walls are derived. Based on these comprehensive numerical results, an empirical relation is derived which is suited for design against bow collisions. This resulting expression for bow collision forces is compared with previously published expressions for ships with ice-strengthening. The derived ship bow collision forces will also be compared with existing standards for modelling ship collisions against bridges published by AASHTO [3] which was developed for US highway bridges over rivers, by IABSE (see Larsen [4]), in connection with the bridges over the Great Belt in Denmark, and by Eurocode [5].
Finally, for design of piers and pylons against localized impact loads, a pressure - area relation for bulbous bow impacts is derived.

2. RISK ACCEPTANCE CRITERIA

The operational risk acceptance criteria for a major bridge must reflect a number of considerations such as:

- The risks of the users of the link shall be reasonable and comparable to other traffic installations and should be justified by its benefits for the people transported, job creation and for the society as a whole.
- The safety shall be optimized by minimization of the risks by appropriate safety measures, taking account of their benefits and costs, and of established good practice.
- The risks should not be overly concentrated on particular individuals or communities.
- The risks of major accidents in the form of for example multiple-fatalities or high costs should be a small proportion of the total.
- The risk shall be systematically managed and evaluated regularly throughout the lifetime of the bridge.

With these considerations in mind, the following types of operational risks related to ship-bridge collisions should be considered and quantified during the design phase and updated at regular time intervals during the operation of bridges:

- Fatalities and injuries to users of the bridge caused by structural failure due to ship impact.
- Disruption of service due to failure of the bridge or reduction in capacity due to ship impacts or structural weakening of the bridge due to fire in ships caught by the bridge.
- Third party risks related to accidental impact to ships passing the bridge, e.g. damage to ships and persons on ships due to collision with the bridge and ship collisions or grounding due to increased navigational complexity.
- Environmental damages due to releases from a ship colliding with the bridge.

Normally the acceptance criteria and the general risk management methodology for major bridges will be based on the ALARP principle. This means that risk shall be reduced as long as the cost of the risk reducing measures is not disproportionate to the effect of the measure. In addition, the risk to users of the bridge should not exceed a level which is unconditionally intolerable chosen such that the level reflects the safety standards elsewhere in the surrounding society.

In the following section, analytical tools will be presented which can constitute elements in a probabilistic procedure for estimation of these operational risks.

3. PROBABILITY OF SHIP COLLISIONS AGAINST BRIDGES

To perform a consistent quantitative risk analysis of new bridge structures exposed to ship collisions, the first step is to collect basic background information such as Seabed bathymetry; Bridge geometry; Bridge alignment; Future road and railway traffic; Wind, current, and ice conditions; Navigational routes; Future ship traffic characteristics and volume; and Spatial distribution of the ship traffic.

Typically, the bridge is designed for a hundred year service life. It is, of course, not possible to predict the ship traffic for this long span of years. The risk analysis must be performed for a shorter period. The future ship traffic forecast estimate can be based on a recording of the present traffic in the region by AIS (Automated Identification System) followed by a prediction for the expected traffic say twenty-five years

from now. Such a prediction can be based on a hearing process with stakeholders in the area about their plans; and a general knowledge of the future global trends in shipping.

To reduce the ship-bridge collision risk, it is most often necessary to improve the navigational channel layout near the planned bridge. The direction of the navigational channel should be close to perpendicular to the bridge line and the location of bends in the navigational channel before the bridge should be arranged such that ships that omit to change course at these bends have a low probability for collision with the bridge.

In international waterways, the right of navigation requires bridges to be constructed such that the navigation is not interfered. To demonstrate such safe navigational conditions, it is crucial to establish a mathematical model for estimation of the required horizontal clearance of the navigation span based on information on the sizes and number of the passing ships. That is, to determine the number of critical meetings in the vicinity of the bridge.

3.1 CRITICAL MEETING SITUATION

One effect of the construction of a bridge over a channel with significant ship traffic is that the ship traffic will be concentrated in narrow shipping lanes and the probability of shipping accidents may increase. The number of ships that have to take evasive actions near the bridge influences the frequency of ship collision accidents near the bridge. Evasive actions often occur in situations where two or more large ships meet in a confined navigational channel. Here we shall describe elements of a model for an empirical estimation of the minimum safety domain in which the navigators feel comfortable when passing other ships or a bridge pylon. The procedure is based on the safety domain concept and will be described by calculation of the frequency of critical meetings or overtaking situations on a certain length interval L_W of the shipping route segment passing under the bridge.

In order to achieve safe navigational conditions, a navigator will try to keep a certain distance between his ship and other vessels and obstacles. For a review of these safety areas, or ship domains, see Szlapczynski & Szlapczynski [6]. Ship domain theory is useful for estimation of the fraction of ships that are capable to sail through a traffic lane at constant speed without getting too close to fixed objects or to other ships.

For free navigation at service speed with no obstructions in a navigational channel, the average ship domains have been identified as an ellipse with a length in the course direction equal to 8.0 L and a length in the side direction of $3.2L$ where L is the ship length, see Fujii & Mizuki [7]. In narrow channels or in harbours where the vessels travel at a reduced speed and where no overtaking or head-on encounters occur, the ship domain is reduced to a length in the course direction equal to 6.0L, and a length in the side direction of $1.6L$.

In case of one way ship traffic, the empirical domain theory suggests a minimum bridge navigational span opening equal to the width of the safety domain for the typical large ship passing the bridge, i.e. either 3.2 or 1.6 times the length L of the ship. Ships with lengths above this ship design size may experience a lack of free navigation since their ship domain ellipse will be wider than the lane width.

For two-way traffic without ship traffic separation, Fig.1 shows conditions related to a critical meeting situation. In this case the ship domains should not touch the bridge pylons or the meeting ships and the navigational span can include a transverse separation zone L_a. Fig.1 shows that the width required when two ships can be present near the bridge is determined as:

$$W_N = \alpha L_1 + 0.5\left(\alpha L_2 + B_2\right) + L_a \tag{3.1}$$

where α = 1.6 or 3.2, L_1 is the length of the longest ship, and L_2 and B_2 are the length and the breadth of the smaller ship.

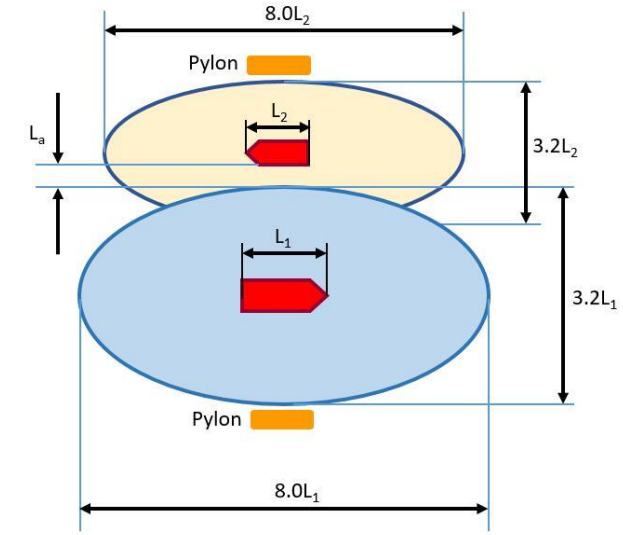

Fig. 1. Two ship critical meeting situations for free navigation without a ship traffic separation zone

For free navigational conditions, the empirical dimensions for the ship domain have been verified by studies of AIS tracks. Hansen et al.[8] used observations from Danish waters of ship-ship encounters and ship-bridge pylon distances to visualize the distances between all ships in the considered areas in special intensity plots. The registrations were displaced to the center of the ships taking into account the actual location of the Global Positioning System (GPS) signal on the ships. All distances were measured from each ship to all other ships and were then normalized with the length L of the current ship. By this method the authors could include ships of all sizes in their analysis. Fig.2 shows observed normalized transverse ship-ship distances. The observed data confirm the ship domain dimensions given in Ref.[7].

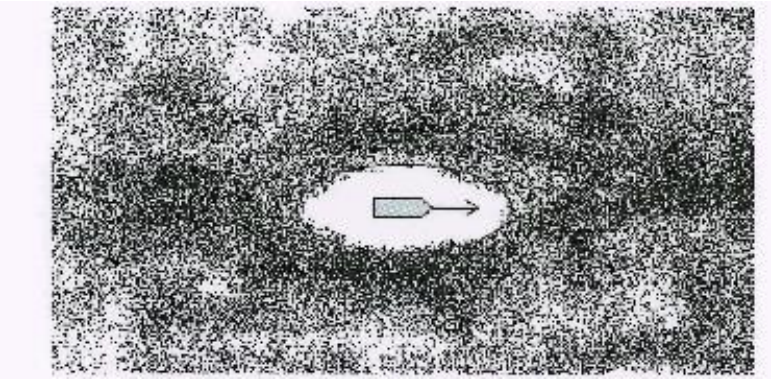

Fig. 2. Normalized distances between ship-ship encounters. (Hansen et. al.[8])

Assuming that the ship traffic in each direction can be described by mutually independent Poisson processes, then the simultaneous occurrence, i.e. meetings of ships in the time interval t on a waterway with length L_w, can also be approximated by a Poisson process with mean and variance given by:

$$E\left[n_m\right] = \alpha_{EW} t \tag{3.2}$$

$$Var\left[n_m\right] = \sigma_{N_m}^2 = \alpha_{EW} t \tag{3.3}$$

Here it can be shown that:

$$\alpha_{EW} = L_w Q_w Q_E \left(\frac{1}{V_w} + \frac{1}{V_E} \right) \tag{3.4}$$

where

α_{EW} is the average number of meeting situations per time unit,

L_w is the distance considered,

Q_w, Q_E are ship movements per time unit, and

V_w, V_E are the average speeds.

Similar expressions can be established for overtaking ships in separate seaways.

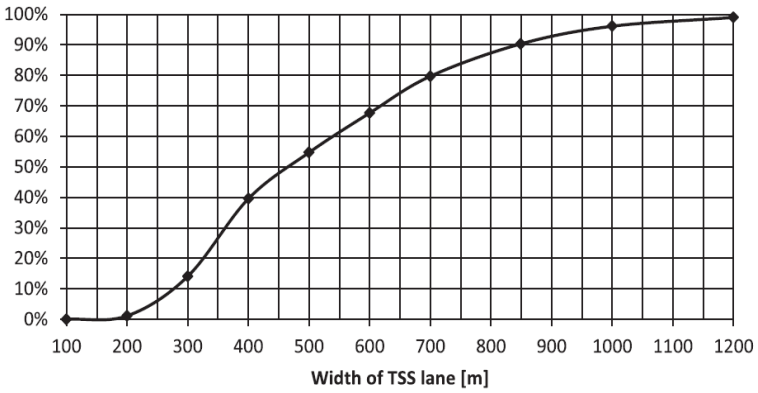

Fig.3. Percentage of co-directional ships with free flow, i.e. without violating the ship domain as function of the width of the traffic lane. (Jensen et al [9]).

In an estimate of the probability of critical meeting situations, it is necessary to use the actual length and speed distributions of the ship traffic and apply a numerical simulation procedure to determine the violation of the safety ellipses. As an example on the application of an encounter simulation analysis, we can consider the results of a calculation for overtaking in one shipping lane in Fehmarbelt conducted by Jensen et al. [9]. The annual traffic in the considered shipping lane consisted of 47,140 ship movements of different ship sizes and ship speeds. The shipping lane L_w is two nautical miles long. Fig. 3 shows the percentage of ships, which have free flow as a function of the width of the traffic lane, i.e. ships where the ship domain given for free flow is not violated by other ships or by the traffic lane boundaries, as function of the lane width. It is seen that a reduction of the bridge span opening and thus the traffic lane width, W , from 850 m to 700 m results in a doubling, from 10% to 20%, of the number of ships with a violated ship domain.

3.2. SHIP - BRIDGE COLLISION PROBABILITY ANALYSIS

A model for estimation of the probability that a ship collides with a bridge structure has been presented in Pedersen et al. [15]. This model was based on a division of the ship-bridge collision probability into a number of different phenomena and subsequent application of mathematical models to quantify the risk from each category. Founded on the same principles, we shall here present a collision probability model, which includes accidents caused by human errors as well as technical factors.

Technical failures where the navigator loses control of speed and course must be included in any probability model for ship collisions. Technical failures can be due to loss of propulsion leading to a drifting ship and/or due to steering machine failure.

However, experience shows that more than 80% of ship collision accidents are due to human errors. A mathematical model for the probability of ship collisions due to human errors is based on calculation of the number of collision candidates in the case of blind navigation, N_a :

$$N_a = N_{ships} \times P_{geometric} \tag{3.5}$$

where N_{ships} is the number of ships on the route in a given time interval and $P_{geometric}$ is the geometric probability that a ship on this route will be on collision course with the bridge structure. The number of possible collision candidates N_a is then multiplied by a causation probability P_c in order to find the actual number of ship collisions P_{col} during the considered time interval:

$$P_{col} = P_c \times N_a \tag{3.6}$$

where the causation probability P_c is the fraction of the accident candidates that results in an accident and models the action of the navigators on board of the ships.

An important part of the estimation of the possible collision candidates, $P_{geometric}$, is the transverse distribution f(z) of the ship traffic in passing the bridge. Studies of AIS tracks can be used to determine the spatial distribution in a given navigational route, and the resulting numerical, or histogram, distributions can be approximated by Gaussian, Lognormal or other analytical distributions, see Figs. 4-5. The parameters in the transverse distribution f(z) estimated from AIS observations can be compared to published empirical expressions for the distribution parameters. Karlson et al. [10] proposed a Gaussian distribution with the standard deviation to be taken as 40% of the width of the navigational channel. Other proposals are given in Larsen [4].

The causation factor P_c depends on a number of sources such as the annual distribution of visibility in the considered area, the competence of the ship crew, the presence of pilots, and the presence of a VTS system in the region. Causation factors P_c in the range of $0.35\times10^{-4} \sim 3.2\times10^{-4}$ have often been used.

The collision frequency estimation can be based on an evaluation of four accident categories:

$$P_{total} = P_{Cat.1} + P_{Cat.2} + P_{Cat.3} + P_{Cat.4} \tag{3.7}$$

These categories are characterised as follows:

Category 1 Includes ship collisions caused by human errors associated with ships which follow the ordinary, straight route at a normal speed and with a normal ship track distribution f(z), see Fig. ~~5~~4. With spatial distributions f(z) modelled as a Gaussian or a Lognormal distribution, there would hardly be any ship traffic distances away from the bridge opening. Therefore, to take into account unusual events and to obtain a certain crashworthiness of the approach spans, it is often assumed that between 1% and 2% of the ship traffic is uniformly distributed across the channel. This will take care of the very rare ship collision accidents which can happen away from the main shipping routes due to gross human errors.

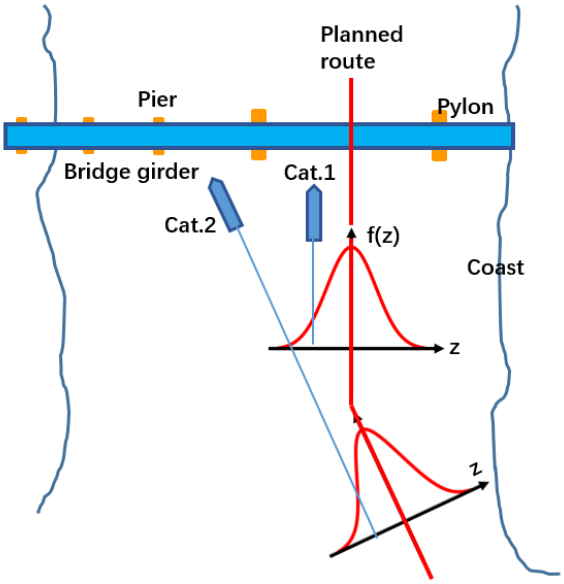

Fig. 4. Ship collision scenarios of Category 1 and Category 2

The calculation of the expected number $P_{Cat.1}$ of collisions per unit time T for a bridge segment between points A and point B, see Fig. 5, can be based on the following expression:

$$P_{Cat.1} = \frac{1}{T} \sum_{\substack{ship \\ class\ i}}^{n} \int_{z=z_a}^{z_b} \int_{0}^{T} P_{c,i} Q_i(t) f(z) dt\, dz \tag{3.8}$$

where

i is the ship class (for instance ships with lengths between 130 and 150 m).

Z is an axis transverse to the shipping route.

Z_a , Z_b denotes integration limits, see Fig. ~~6~~5

$P_{c,i}$ is the causation factor, i.e. the probability of a collision if the ship is on collision course.

Q_i is the number of ships of class i per time unit (Q_i could for instance be the number of ships with lengths between 130m and 150m).

f(z) is the lateral ship distribution

To reduce Category 1 accidents, it is necessary to arrange fairways and the bridge layout such that there are margins for minor errors and faults on board of the passing ships and to ensure that the ship domains are not violated too often due to insufficient navigational spans.

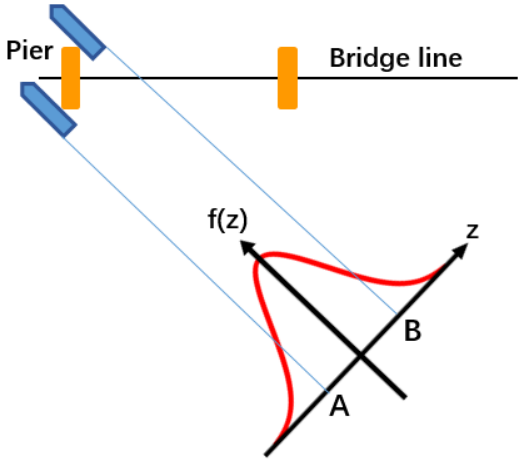

Fig. 5. Ships positioned between $A = Z_a$ to $B = Z_b$ can collide with the considered bridge pier

Category 2 includes those ships which fail to make a proper change of course at a turning point in the vicinity of the bridge. See Fig.4. In this case the ship will continue on the old course until the ship navigator corrects the course, the ship goes aground, or the ship reaches the bridge line and may collide with the bridge.

The Category 2 event can be modelled by inclusion of the probability, P_0 , for omission of a course change:

$$P_{Cat,2} = \frac{1}{T} \sum_{\substack{n \\ ship \\ class\ i}} \int_A^B \int_0^T P_0 P_{c,i} Q_i f(z) dt\, dz \tag{3.9}$$

The probability that a ship fails to change course at a turning point can for example be modelled by:

$$P_0 = P_t + (1 - P_t) \times P_d^{\frac{d-a}{a}} \tag{3.10}$$

where P_t is the probability that the navigators continue on the wrong course and completely neglect the needed course change and P_d is the probability of omission to check the position of the ship, d is the distance sailed on the wrong track and a is the average sailing length between position checked by the navigator.

The Category 2 hazard shows that it is necessary to consider carefully the layout of sailing routes near the bridge in order to reduce as far as possible the probability that ships that neglect a turn will collide with the bridge.

Category 3 includes ships that do not follow the ordinary route recommended in navigational charts due to technical errors such as ships drifting due to mooring or anchoring failures, drifting ships at work such as fishing vessels, ships drifting due to loss of propulsion, ships in pack ice drifting against the bridge, and ships with a steering gear failure.

For ships, drifting due to loss of propulsion, it is normally assumed that the ships at the time of engine failure are located on the idealised sailing route. Rasmussen et al. [11] give suggested probabilities for loss of propulsion and for loss of control for a typical commercial ship:

$$P_{Loss\ of\ propulsion} = 1.5\times10^{-4} \text{ failures per hour, and}$$

$$P_{rudder\ failure} = 6.3\times10^{-5} \text{ per vessel and hour.}$$

Within a relatively short time span, the crew can normally repair the loss of propulsion or loss of control. Rasmussen et al. [11] give an empirical estimation of the probability of drifting as function of time by the complementary distribution function of the repair time distribution. The distribution function for self-repair $P_{repair}(t)$ can be approximated by a Weibull function with k = 0.5 (shape) and λ = 0.605 (scale):

$$P_{drift}(t) = 1 - P_{repair}(t) = e^{-\left(\frac{t}{\lambda}\right)^k} \tag{3.11}$$

The moving direction of a drifting ship depends on wind and current directions. Typically the drifting ship will be oriented such that the longitudinal axis of the ship is transverse to the moving direction.

Drifting ships and ships without control can collide with the bridge structure at any point along the bridge line, while excluding areas with low water depth, where grounding can occur before hitting the bridge. If the water depth is not too deep then the navigator may be able to stop the drifting by use of the ship's anchoring system.

The number of collisions due to drifting depends on the wind and current directions and velocities. As an example, the collisions due to drifting can be determined by an expression of the following type:

$$P_{drift}^{bridge} = \frac{1}{T}\int_0^T \sum_{ship\ class\ i} Q_i \left(1 - P_{anchor}\right) \int_{\theta=0}^{360} P_{wind,current}(\theta) \sum_{segments} P_{technical\ error}(L_w)$$

$$\int_{z=0}^{L_w} \int_{V_{drift}} P_{drift}\left(t_{col} / X\right) f\left(V_{drift}\right) dV_{drift}\, dz\, d\theta\, dt \tag{3.12}$$

Here P_{anchor} is the probability of a successful anchoring in a propulsion failure situation, $P_{wind,current}$ represents the probability of having the drifting direction θ. The drifting speed is given by $f\left(V_{drift}\right)$ and X defines the parameters which give the time to collision.

When a steering system fails, the rudder will be locked and the ship will start sailing in a circular path. The diameter depends on the locked position of the rudder and the under-keel clearance. Low water depth will increases the turning diameter. Often the rudder will be locked in an extreme position and the ship may go into a circular path, and provided a large under-keel clearance, with a diameter equal to two to three times the ship length.

Category 4 includes ships, which make evasive manoeuvres near the bridge due to the presence of other vessels and because of such manoeuvres, collide with the bridge. The number of multiple critical encounters can be estimated based on the ship domain simulations described in Section 3.1.

If the bridge span opening is sufficiently wide with good margins for evasive manoeuvres and if the number of critical encounters near the bridge are infrequent, then this risk contribution is normally relatively insignificant.

The procedure presented here for estimation of the collision frequency depends on some empirical and uncertain factors such as the lateral distribution f(z) of the ships, the causation factor P_c, the probability P_0 of omitting a course change in a fairway, etc. For this reason, the mathematical model should be verified by a comparison between a prediction of the number of collisions and grounding events predicted by this model and the number of actual incidents over a period in the region.

3.3 SELECTION OF DESIGN VESSELS

Using a procedure as the one described in Section 3.2, it is possible to determine the probability of collision for each pier or bridge girder segment caused by the individual ship class "i" . See Table 1.

Table 1. Annual collision frequencies P_{total} for different bridge components

Frequency [Annual]	Ship Size Class									Total
	1	2	3	4	5	6	7	8	9	
Pylon 1	3.64E-03	1.27E-04	5.55E-05	5.45E-05	1.28E-05	5.78E-06	3.90E-06	6.29E-07	3.58E-07	3.90E-03
Pylon 2	8.14E-03	4.04E-04	1.60E-04	1.14E-04	3.56E-05	1.60E-05	8.96E-06	2.43E-06	7.66E-07	8.89E-03
Pier 4	1.56E-03	8.11E-04	2.72E-04	1.91E-04	7.30E-05	5.04E-05	2.63E-05	5.75E-06	1.98E-06	2.99E-03
Pier 5	1.32E-03	7.45E-04	4.57E-04	3.32E-04	1.19E-04	9.75E-05	3.95E-05	1.50E-05	2.58E-06	3.13E-03

From this estimate of the annual frequency of ship collisions with the different ship size classes "i" to the various bridge structural elements, one or more "design vessels" can be determined. The design vessel for an individual bridge element is defined as a striking vessel, the bridge structural element must withstand without critical failure in order for the total bridge line to fulfil the design criteria. A typical acceptance criterion for the bridge structure related to the availability of the bridge for traffic could be that the annual frequency for collapse of the bridge or disruption of the bridge traffic for an extended period shall be less than 10^{-4}. That is, in order for the acceptance criteria to be met for the whole bridge line, impacts from all ships equal to or smaller than the sizes of the design vessels should not lead to critical failure of any of the bridge elements. It is up to the bridge designer to choose an optimum distribution of the survival probability for the individual structural elements.

The consequence or severity of the collision is modelled by a severity, or Heinrich [12], factor that can be used to give the ratio between impact incidents that cause critical failure and all incidents, which have the potential to cause critical failure. Thus, even if the bridge element is subjected to a ship impact with a ship larger than the design ship for that specific structural component, then there is a certain probability that the bridge element does not collapse. This may be due to two effects:

1) The actual impact speed and thus the kinetic energy of the colliding ship at the moment of impact is reduced due to last minute's ship maneuvers or because the impact at for example a bridge pier is not a central impact and will result in sliding along the pier surface, and
2) The bridge elements have a reserve capacity above the estimated capacity of the elements.

Due to these modifying effects, the probability for a critical ship collision against a pier can be expressed as:

$$P_{Critical\ failure} = P_{Critical\ failure/Collision} \times P_{Collision} \tag{3.13}$$

Where $P_{Collision}$ is the probability for a collision with a ship larger than the design ship and $P_{Critical\ failure/Collision}$ is the factor which describes the probability that a given collision from a ship larger than the design ship causes critical failure of the bridge element.

An accurate calculation of $P_{Critical\ failure/Collision}$ is difficult because of many uncertainties and varying conditions that would have to be considered in practice. As mentioned above, then the momentum and the kinetic energy transferred to the bridge element by the impacting design ship has a certain probability to be less than the momentum and energy estimated simply from an assumed service speed and central collision scenario. Lützen [13] made a survey of ship–ship collisions and found that the reported speed of the striking vessels at the moment of impact is reduced and often can be assumed to be uniformly distributed between a very low speed and the service speed. A reduction in collision speed will have a relatively large impact on the resulting collision energy.

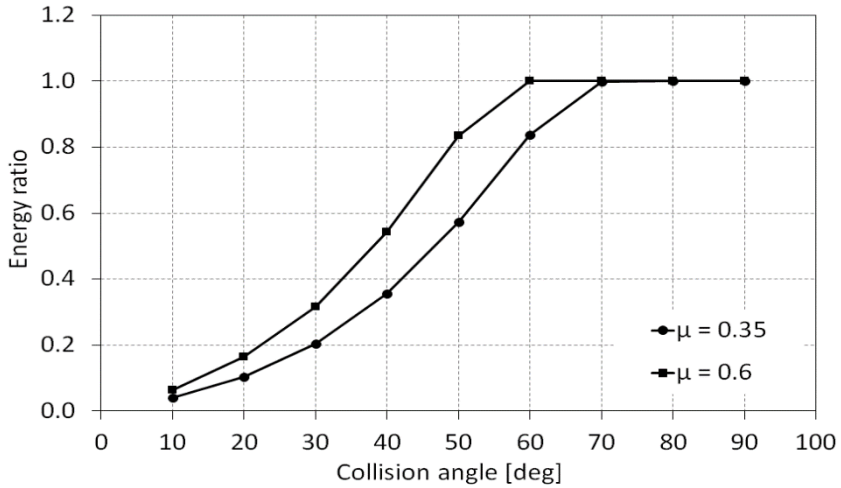

Fig. 6. Energy loss ratio of a vessel colliding with a rigid wall with as function of the collision angle and coefficient of friction μ. Ref. [14]

The impact location and the impact angle may also be influential such that not all the kinetic energy of the striking vessel will be available for crushing of the bridge or the ship. The most critical collisions will be head-on collisions perpendicular to the surface of the bridge pier. For smaller impact angles, sliding can occur between the ship and the bridge pylon or pier. In this case the energy released for crushing depends on the collision angle and the coefficient of friction μ. See Fig. 6.

Similarly, for drifting ships, the full kinetic energy will only be released for crushing against pylons and piers in the low probability event of a central collision where the ship is completely stopped by the impact.

An exact calculation of the severity or Heinrich factor from ship impact speeds and locations is not possible. However, a conservative factor can be estimated when only the ship speed and impact locations can be relied upon. The AASHTO guideline [3] gives severity or Heinrich ratios as function of the ratio between the ultimate lateral resistance of a pier and the vessel impact force. Table 2 shows an example of design vessels for a bridge.

Table 2. An example of design ships and energies for different bridge components

	Design ship - normal speed			Design ship – drifting		
Bridge component	Length [m]	Speed [m/s]	Energy [MJ]	Length [m]	Speed [m/s]	Energy [MJ]
Pylon 1	120	6	170	235	1	35
Pylon 2	130	6	180	240	1	37
Pier 4	90	6	70	200	1	17
Pier 5	85	6	60	200	1	17

Having determined the size and speed of a selection of "design vessels" that each bridge pier and pylon shall withstand without critical failure, the next step is to determine the forces these ships will exert on the structural elements.

4. CONSEQUENCE ESTIMATION

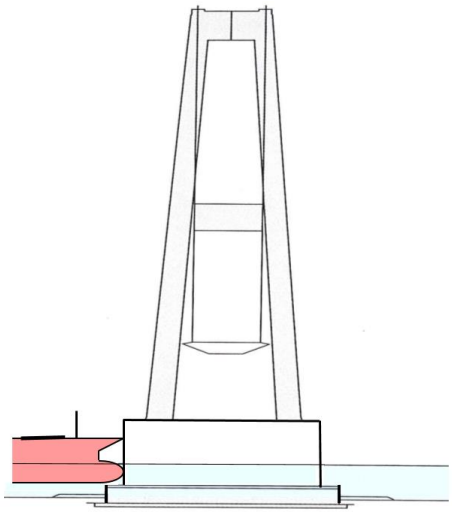

Fig. 7. Head-on collision against pylon

To estimate the consequences of ship collisions against bridge structures, a twostep approach can be applied.

a) In the first step, a detailed local structural force-deformation analysis is performed. That is, derivation of the forces associated with crushing of the ship structure against a rigid bridge structural element to get force-deformation relations for bow impacts, see Fig. 7. For side impacts, and deck house impacts, force-deformation relations can be determined using explicit finite element analyses or by semi-analytical methods based on a summation of the resistance of an assembly of structural strength components in the ship structure, see Ref. [15].

At the design stage, it is neither possible nor necessary to identify the structural design or other details of the future striking vessels. For this reason, it is not important to perform very detailed comprehensive time and cost consuming non-linear finite element crushing calculations. It is often sufficient to use simplified procedures, which can give expressions for mean and variance values of the crushing forces for the design ship sizes.

b) The second step in the approach for a comprehensive consequence analysis is to apply the force-displacement curve obtained in Step 1 as a non-linear spring to represent the stiffness of the ship structure in a global dynamic model in order to estimate the overall deformation of the bridge structure. For gravity supported piers or pylons, it is in Ref. [16] shown that provided some small foundation displacements can be allowed then the impact capacity of the piers or pylons can be improved. For situations where the inertia

of the piers can be neglected, an analysis of the effect of flexibility for pile supported piers is presented by Hoang and Lützen [17]. For floating bridge structures, the global response analysis shows that a major part of the available collision energy can be transferred to dynamic response of the bridge structure, see Sha et al. [18].

4.1 BOW CRUSHING FORCES

It is possible to estimate bow crushing forces by Non-linear Finite Element Analyses (NLFEA). See Sha and Hao [19]. However, due to the localized nature of the folds in the crushing modes, a very fine mesh size is required with element length of the order of a few plate thicknesses, see Chen et al. [20]. For the large and complicated ship bows, this is a difficulty. Another, challenge is the major role played by contact forces in the final crushing modes. For these reasons, we shall here apply simplified methods, which have been verified by experiments [21] and [15].

A variety of simplified formulas have been proposed in the literature in order to estimate the mean crushing forces of plated structures such as ship bows. The procedures are all based on evaluation of crushing loads for a sequence of cross sections of the ship section. See Fig. 8. Although these formulas are based on the same rigid-plastic material modelling procedures, they are in reality different due to different assumed folding mechanisms.

Theories based on intersection elements such as L, T and X type elements, see Fig. 8, as well as theories based on plate unit elements have been applied to determine the axial crushing of bulbous bow structures. With reference to the upper bound theorem, the mean crushing force is in most published simplified procedures derived by dividing the total absorbed energy by the crushing distance while assuming kinematically admissible crushing mechanisms. That is,

$$P_m = \frac{E}{2H \cdot \eta} \tag{4.1}$$

where P_m denotes the mean crushing force, E is the absorbed energy during one fold crushing distance, H is the half folding length and η is the dimensionless effective crushing distance. In most cases, the energy is a function of the unknown variable H. The value of H and the associated mean crushing force P_m are derived by minimizing the mean crushing force:

$$\frac{\partial P_m}{\partial H} = 0 \tag{4.2}$$

Often P_m is a function of more than two variables describing the folding patterns such as I and J. When this is the case, these variables are determined from the optimality criterion:

$$\frac{\partial P_m}{\partial H} = 0,\ \frac{\partial P_m}{\partial I} = 0,\ \frac{\partial P_m}{\partial J} = 0, \ldots \tag{4.3}$$

Results obtained by these different simplified analysis procedures were in Ref. [21] compared with those observed from large-scale quasi-static bow crushing experiments. The conclusions derived from that study was that Yang & Caldwell's method in Ref. [22] and a slightly modified method by Amdahl, Ref. [23], give relatively good predictions of the experimental crushing forces.

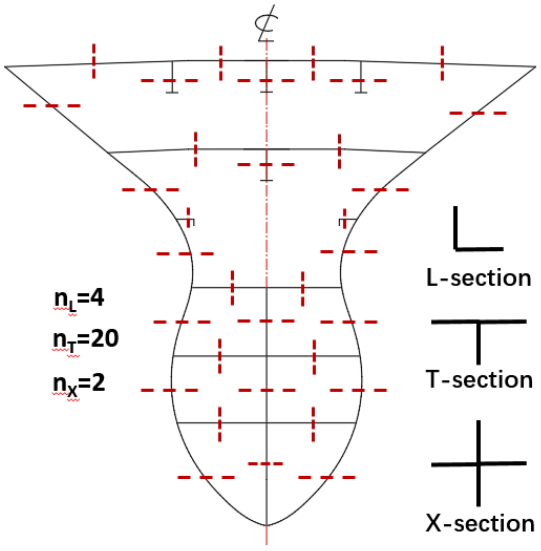

Fig. 8. Subdivision into Intersection Unit Elements. L-, T- and X- type elements [15]

Amdahl [23] derived the following closed formula for the mean axial crushing force P_m of bow models collapsed axially in quasi-static conditions:

$$P_m = \sigma_c A = 2.42\sigma_0 A\left[\frac{n_{LT}t^2}{A}\right]^{0.67}\left[0.87+1.27\frac{n_X+0.31n_T}{n_{LT}}\left(\frac{A}{(n_X+0.31n_T)t^2}\right)^{0.25}\right]^{0.67} \tag{4.4}$$

Here σ_0 denotes the ultimate stress, A is the sectional area of the crushed section, t is the mean thickness of the plate, n_X is the number of X type elements, n_T is the number of T elements and n_{LT} is the number of L and T elements, as indicated in Fig. 8. The effective crushing distance is taken as η =0.85 times the folding length in case of transversely stiffened structures, and the effective crushing distance in case of longitudinally stiffened structures is η = 0.75 times the folding length. The angle elements at the intersection of the upper deck and the outer shell are included as half of the X elements. See Ref. [15].

Yang & Caldwell [22] developed similar simplified formulas for crushing forces for L-, T- and X- type elements assuming four types of basic deformation mechanisms. Their expression for the crushing force is as follows:

$$P_m = \sigma_0(1.178/H\sum^{n_1} b_i t_i^2 + 0.215H\sum^{n_{AT}} t_i + 6.935\sum^{n_{AT}} t_i^2 + 0.265H\sum^{n_T} t_i$$

$$+0.589\sum^{n_T} t_i^2 + 0.75H\sum^{n_c}\sum^{4} t_i + 0.375\sum^{n_c}\sum^{4} t_i^2) \tag{4.5}$$

where P_m is the mean crushing force, σ_0 is the flow stress (mean value of the yield stress and ultimate stress), b_i is the width of flange, t_i is the thickness of the plate, H is the folding length, n_c is the number of the X element, n_T is the number of the T element, n_{AT} is the number of the L and T element, n_1 is the total number of the L,T and X element.

Here the effective crushing distance η is taken to be 2/3 times the folding length. When the folding length H is greater than the frame spacing, the frame spacing will be used as the folding length.

The strain rate effect due to the dynamics in a ship collision is modelled by Cowper-Symonds' [24] empirical expression

$$\frac{\sigma_{\mathrm{d}}}{\sigma_0} = 1 + \left(\frac{\dot{\varepsilon}}{C} \right)^p \tag{4.6}$$

$$\dot{\varepsilon} = \frac{V}{u} \tag{4.7}$$

where σ_{d} is the dynamic stress, σ_0 is the flow stress, V is the ship speed in longitudinal direction, u is the frame spacing. For mild steel, C=40.4 and p=0.2 is applied and for high tensile steel, we use C=3200 and p=0.2 as proposed by Paik and Thayamballi [25].

In the numerical calculations, we shall determine the decreasing kinetic energy of the striking ship as function of the crushing distance and this kinetic energy is then used to determine the reduced speed V and thus the strain rate as function of the crushed distance. Especially for ship structures built from mild steel, this strain rate effect is important.

4.2 CALCULATED MAXIMUM BOW CRUSHING FORCES

The bow crushing forces for six ships of different sizes are investigated in order to obtain the crushing force in head-on collisions against a rigid wall. The vessels chosen are a 5800DWT bulk carrier, a 12800DWT tanker, a 25000DWT container ship, a 45000DWT bulk carrier, a 53500DWT bulk carrier, and a 70000DWT container ship. The detailed scantlings of the bow structures of these ships are shown in the Appendix.

By using the methods of Amdahl [23] and Yang & Caldwell [22], the number of L, T, and X elements in each cross section of the bulbous bow are counted, and the mean crushing forces are calculated for each frame in fore body by adding up the loads of these structural elements. As mentioned above, decreasing velocities are applied in the strain rate relation for the flow stress to take into account the effect of the strain rate.

In some of the ships, the tip of the bulbous bow is so stiff that for a given force a section further aft in the bow will collapse firstly. In such cases, the sections are re-arranged such that the force-displacement relations become monotonically increasing.

As ~~a~~ first step, the crushing forces have been determined for all the six vessels using both the modified Amdahl method and the Yang and Caldwell method. Fig. ~~15~~9 shows the result from two of these calculations. It is noted that the differences between the modified Amdahl method, Eq. (4.4), and Yang & Caldwell's method, Eq. (4.5), are not significant.

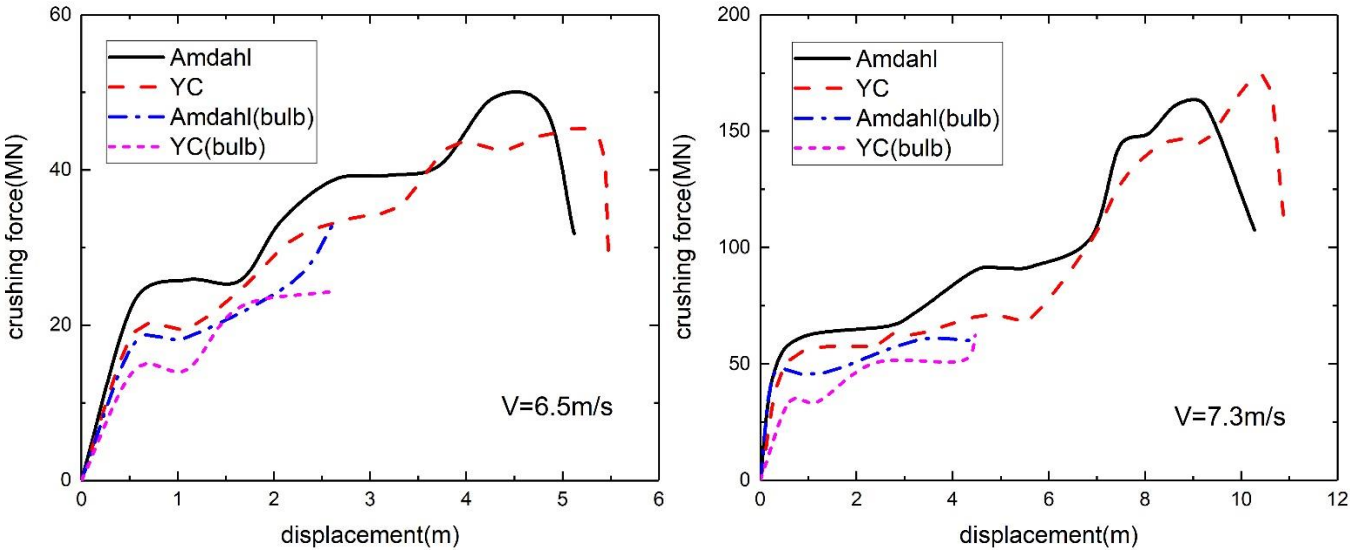

(a) Crushing force of 5800DWT bulk carrier (b) Crushing force of 25000DWT container ship

Fig.9. Crushing force of two different ship sizes using two calculation methods

Fig. 16 shows the effect of the initial ship speed for the force-displacement relations obtained using Amdahl's method, Eq. (4.4). It is seen that for the same indentation the crushing forces do not differ much with the initial ship speed. However, due to the variation of the initial kinetic energy, the crushing distances differ.

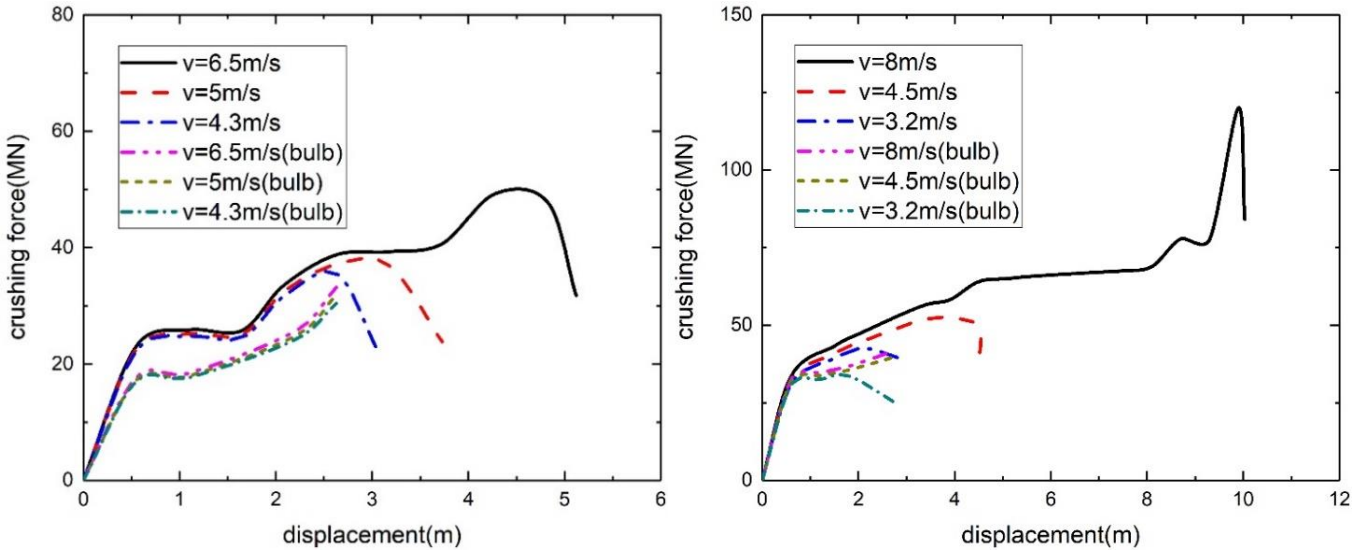

(a) Crushing force 5800DWT bulk carrier. (b) Crushing force 12800DWT tanker.

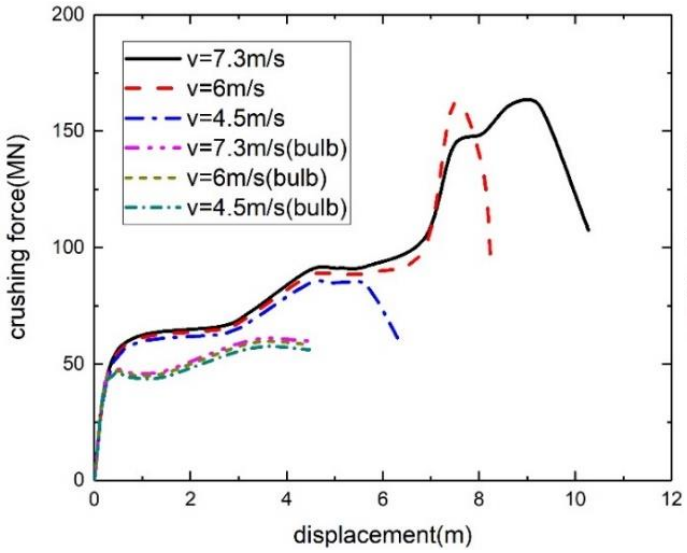

(c) Crushing force 25000DWT container ship

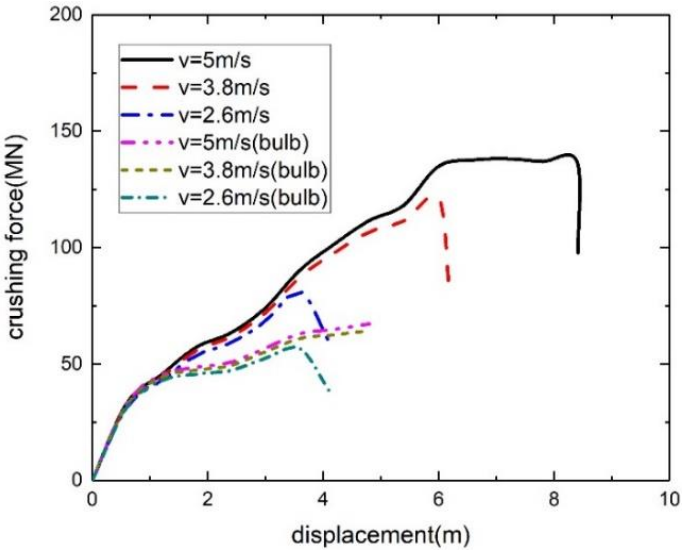

(d) Crushing force 45000DWT bulk carrier.

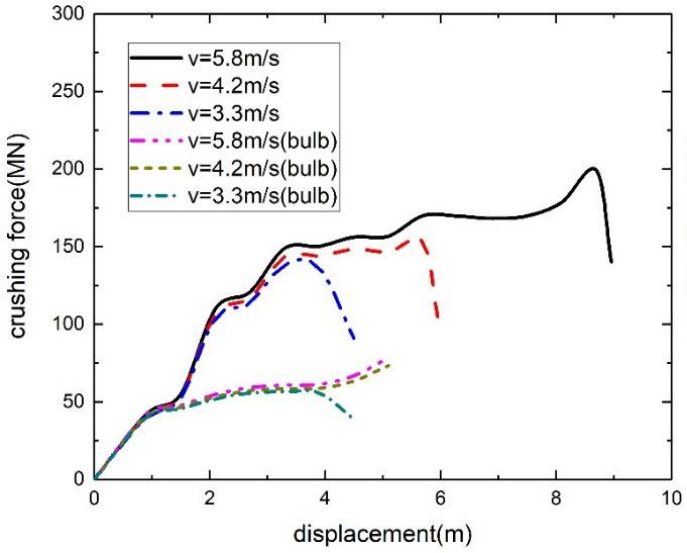

(e) Crushing force 53500DWT bulk carrier

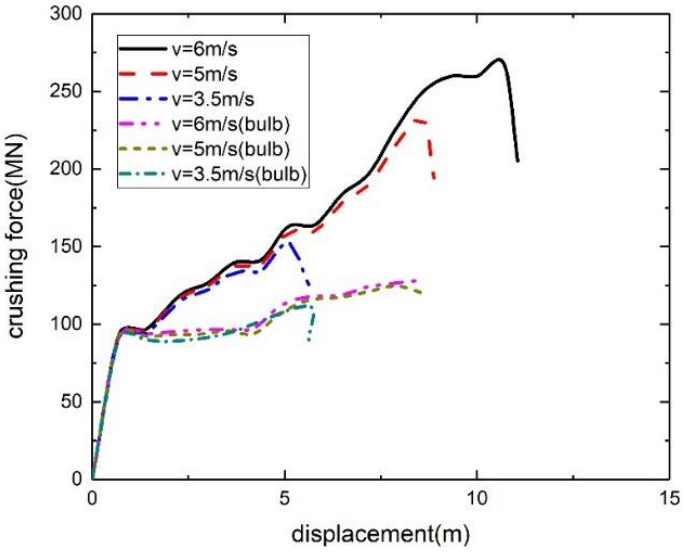

(f) Crushing force 70000DWT container ship

Fig.10. Crushing force for six different ship sizes with different velocities by use of Eq (4.4)

4.3 EMPIRICAL METHOD FOR MAXIMUM BOW CRUSHING FORCE

The numerical results presented above show that the governing parameters for the force-displacement relations are the kinetic energy given by the displacement and the initial impact velocity, and the length of the vessel. With this knowledge and based on the calculated force-displacement curves for the six ships, an empirical formula is obtained for the maximum crushing force:

$$P_{bow} = \begin{cases} P_r \bar{L}^{0.45}\left[\bar{E} + \left(1.5 - \bar{L}^{-0.1}\right)\bar{L}^{3.6}\right]^{0.5} & \bar{E} \geq \bar{L}^{3.5} \\ 1.22 P_r \left(\bar{E}\bar{L}\right)^{0.5} & \bar{E} < \bar{L}^{3.5} \end{cases} \tag{4.8}$$

Here we have chosen to apply the same non-dimensional parameters as those used in Ref. [15], i.e. $\bar{E} = \frac{E}{1425} = \frac{0.5mV^2}{1425}$, $\bar{L} = \frac{L_{PP}}{275}$, $P_r = 230MN$, m is the mass of the ship with 5% added mass(10^3t), V is the initial velocity before collision (m/s), L_{PP} is the ship length (m), E is the kinetic energy before collision (MJ), and P_{bow} is the maximum crushing force of the bow (MN).

If the relationship between the crushing force and the displacement is approximated with a parabolic relation, the following expression can be obtained:

$$m\ddot{s} + P_{bow}\sqrt{\frac{s}{s_{\max}}} = 0 \tag{4.9}$$

Using the energy balance, the maximum displacement $S_{\max}$ and collision duration T can be found as:

$$S_{\max} = 1.5\frac{E}{P_{bow}} \tag{4.10}$$

$$T = 1.53\frac{S_{\max}}{V} \tag{4.11}$$

Pedersen et al. [15] presented a similar empirical expression for estimation of the maximum crushing force by investigating the crushing force for six different size ships, all with high ice-class. The effect of strain rate, ship size and the initial velocity were also considered in this analysis. The expressions for the maximum collision force P_{bow}, maximum displacement $S_{\max}$ and collision duration T were given as follows:

$$P_{bow} = \begin{cases} P_0\bar{L}[\bar{E} + (5.0 - \bar{L})\bar{L}^{1.6}]^{0.5} & \bar{E} \geq \bar{L}^{2.6} \\ 2.24P_0[\bar{E}\bar{L}]^{0.5} & \bar{E} < \bar{L}^{2.6} \end{cases} \tag{4.12}$$

$$S_{\max} = \frac{\pi}{2}\frac{E}{P_{bow}} \tag{4.13}$$

$$T = 1.67\frac{S_{\max}}{V_0} \tag{4.14}$$

Where $P_0 = 210MN$.

Identical expressions for the maximum bow crushing forces (4.12), displacements (4.13), and collision durations (4.14) have been adopted by IABSE [4] and by EUROCODE [5] for a speed of 5 m/s. In the recommendations by IABSE and by EUROCODE, these expressions are used for all ships, i.e. not restricted to ice-strengthened vessels.

Another recommendation for evaluation of the crushing force has been presented in the US-Guide issued by AASHTO [3]

$$P_{bow} = 0.12V(DWT)^{0.5} \tag{4.15}$$

Here P_{bow} is the equivalent static impact force (MN), V is the velocity of the ship (m/s) and DWT is the ship dead weight(t). The AASHTO expression (4.15) is independent of the loading conditions of the ships.

To compare the present empirical expressions for the maximum bow crushing forces with the calculated results in Fig. 10 and with the existing recommendations by AASHTO, Eq. (4.15), IABSE and EUROCODE, Eqs. (4.12) – (4.14), the formulas (4.8), (4.10), and (4.11) are used to estimate the maximum crushing force P_{bow} , maximum displacement S_{max} and collision duration T of the considered six ships under full load conditions. The results are presented in Table 3.

It is seen that the proposed empirical expressions (4.8), (4.10), and (4.11) represent the results for the present normal ships without ice-class shown in Fig. 10 very well. It is also seen that the expressions presented in Pedersen et al. [15] for ships with high ice class and adopted by IABSE and by EUROCODE are highly conservative for normal ships, especially for larger vessels. For smaller ships like the 5800DWT bulkcarrier, the AASHTO formula gives an acceptable estimation, however, for the larger ships like the 70000DWT container ship, the maximum bow crushing force results given by AASHTO are too small.

Table 3a Maximum crushing force, displacement and collision time of ships at different speeds under full load

Size	5800DWT bulk carrier			12800DWT tanker		
L(m)		88.4			135	
B(m)		15.6			20.8	
D(m)		6.85			11.2	
m(t)		8151.15			18585	
V(m/s)	6.5	5	4.3	8	4.5	3.2
P(MN)（Fig.10）	**49**	**37**	**36**	**130**	**52.3**	**42.5**
S_{max}(m)（Fig.10）	5.3	3.73	3.05	10	4.5	2.8
P_{bow}(MN) Eq.(4.8)	49.2	38.5	33.6	112	67	50
S_{max}(m) Eq.(4.10)	4.5	3.6	3.2	7.3	4.5	3.4
T(s) Eq.(4.11)	1.06	1.11	1.14	1.4	1.52	1.62
P(MN)（US-Guide）	**59.4**	**45.7**	**39.3**	**108.6**	**61.1**	**43.4**
IABSE & EUROCODE Ice-classed vessel:						
P_{bow}(MN)（Eq. 4.12）	**63.4**	**61.6**	**60.9**	**140.7**	**119.8**	**85.2**
S_{max}(m) （Eq. 4.13）	4.3	2.6	2	6.64	2.47	1.75
T(s) （Eq. 4.14）	1.1	0.87	0.75	1.4	0.92	0.92

Table 3b Maximum crushing force, displacement and collision time of ships at different speeds under full load

Size	25000DWT container			45000DWT bulk carrier		
L(m)	169.4			172.08		
B(m)	27.2			32.26		
D(m)	14.2			16.3		
m(t)	37873.5			63149.1		
V(m/s)	7.3	6	4.5	5	3.8	2.6
P(MN)（Fig.10）	**167**	**136**	**84.6**	**152**	**121**	**81**
S_{max}(m)（Fig.10）	10.6	8.3	6.4	8.7	6.2	4.1
P_{bow}(MN) Eq.(4.8)	**164**	**138**	**109**	**149**	**118**	**86**
S_{max}(m) Eq.(4.10)	9	7.4	5.7	7.9	6.1	4.3
T(s) Eq.(4.11)	1.86	1.9	1.94	2.42	2.47	2.54
P(MN)（US-Guide）	**138.5**	**113.8**	**85.4**	**127.3**	**96.7**	**66.2**
IABSE & EUROCODE Ice-classed vessels:						
P_{bow}(MN)Eq. (4.12）	**213.6**	**204**	**191.5**	**212.7**	**203**	**144**
S_{max}(m) Eq.(4.13）	7.4	5.2	3	5.8	3.5	2.3
T(s) Eq. (4.14）	1.7	1.46	1.17	1.95	1.55	1.5

Table 3c Maximum crushing force, displacement and collision time of ships at different speeds under full load

Size	53500DWT bulk carrier			70000DWT container		
L(m)	182			280		
B(m)	32.26			40		
D(m)	17.2			14		
m(t)	70675.5			102900		
V(m/s)	5.8	4.2	3.3	6	5	3.5
P(MN)（Fig.10）	**203**	**153**	**138**	**268**	**233**	**152**
S_{max}(m)（Fig.10）	9.2	6	4.5	12	8.9	5.6
P_{bow}(MN) Eq. (4.8)	**185**	**141**	**116**	**314**	**269**	**188**
S_{max}(m) Eq.(4.10)	9.4	7	5.5	9.2	7.6	5.5
T(s) Eq.(4.11)	2.5	2.53	2.55	2.36	2.32	2.39
P(MN)（US-Guide）	**161**	**116.6**	**91.6**	**190.5**	**159**	**111**
IABSE & EUROCODE Ice-classed vessels:						
P_{bow}(MN) Eq.（4.12）	**244**	**227**	**199**	**497**	**451**	**316**
S_{max}(m) Eq. (4.13）	7.7	4.3	3	5.86	4.5	3.1
T(s) Eq. (4.14）	2.2	1.7	1.54	1.63	1.5	1.5

In order to illustrate graphically the influence of ship size, Fig. 11 shows the maximum crushing force as functions of DWT tonnage and Fig. 12 shows the maximum crushing force as function of length for fully loaded ships with a speed of 5m/s.

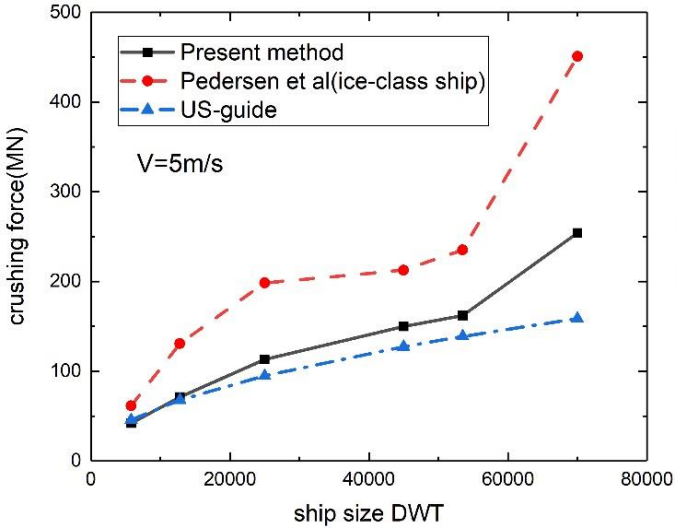

Fig.11. Crushing force for fully loaded ships

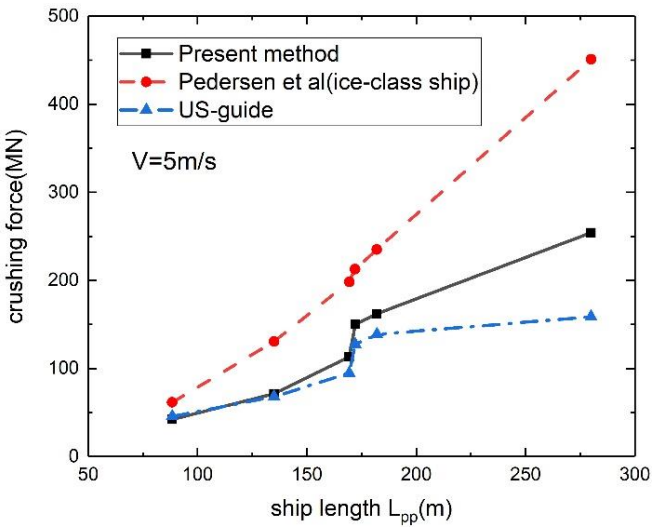

Fig.12. Crushing force for different ship lengths

Minorsky [26] proposed in 1959 an empirical formula ($E(MJ) = 47.2R_T(m^3) + 32.7$) to evaluate the energy of ship collision using the damaged material volume. In order to include an effect of the structural arrangement and the steel properties, Pedersen and Zhang [27] revised Minorsky's formula for bow collisions as follows:

$$E = 3.5(\frac{t}{b})^{0.67}\sigma_0 R_T \tag{4.16}$$

$$F_m = 3.5(\frac{t}{b})^{0.67}\sigma_0 A_m \tag{4.17}$$

where E is the energy absorption of the ship bow, t is the average thickness of the plates, b is the average width of the plates in the cross-section, σ_0 is the flow stress, R_T is the damaged material volume; F_m is the mean crushing force, A_m is the material cross-sectional area.

Figure 13 shows the relationship between the damage material volume and the energy absorption of the bows on the six ships. These results are based on the calculated results shown in Fig. 10. It is seen that Minorsky's original formula gives significantly smaller energy absorption than found from the present calculations, whereas the Pedersen and Zhang‘s formula (4.16) for this case gives reasonably good predictions.

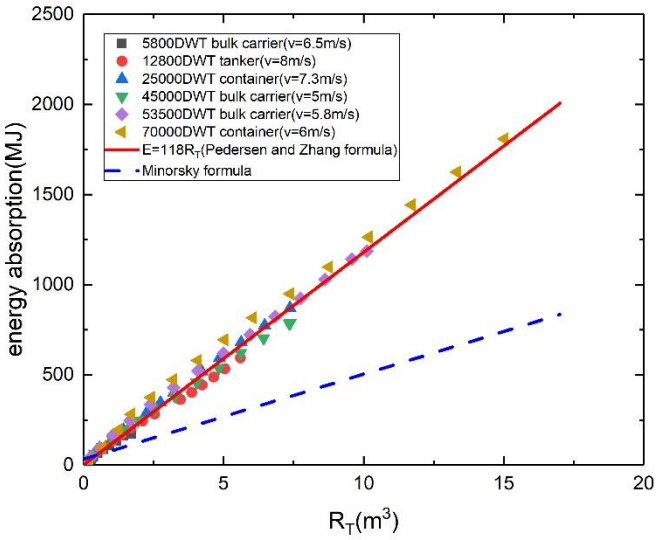

Fig.13. Energy absorption versus damaged material volume

4.4 LOCALIZED BULBOUS BOW COLLISION LOADS

For the design of bridges against ship impacts, not only the total force-deflection relations are relevant but also the more local contact pressure between the colliding vessel and the bridge structure is needed. For offshore structures, recommendations for localized impact loads from ship impacts have been given by Det norske Veritas in DNV RP-C204 [28] and for supply vessel stern end impacts by NORSOK in N-004 [29].

More recently Storheim and Amdahl [30] have re-examined these recommendations. They have used non-linear finite element calculations to determine the average maximum bulbous bow pressure versus contact area for a 7500 ton supply vessel against a rigid flat wall. They propose the following empirical relation between the pressure load p in MPa and the area A in m^2:

$$p = 12A^{-0.7} \tag{4.18}$$

The shape of the contact area is approximately an ellipse and the finite element analysis shows that the simulated contact forces occur over limited areas around the bulb perimeter while the areas in the bulb centre are not in constant contact.

A typical supply ship with a displacement of 7500 tons and a length of 90 m will have a bulb plate thickness of 12.5 mm and bulb bulkhead and deck plate thicknesses of 9 to 10 mm. See Yu & Amdahl [31].

These bow scantlings are smaller than the scantlings to be expected from the bows of ocean going merchant ships. To study the pressure-area relationships of the bulbous bows, Fig. 14 shows the pressure as function of the outer bulb cross-sectional area A_w as well as the pressure as function of the material cross-sectional area A_m. The crushing stresses in Fig. 14 are the mean values considering the strain rate effect.

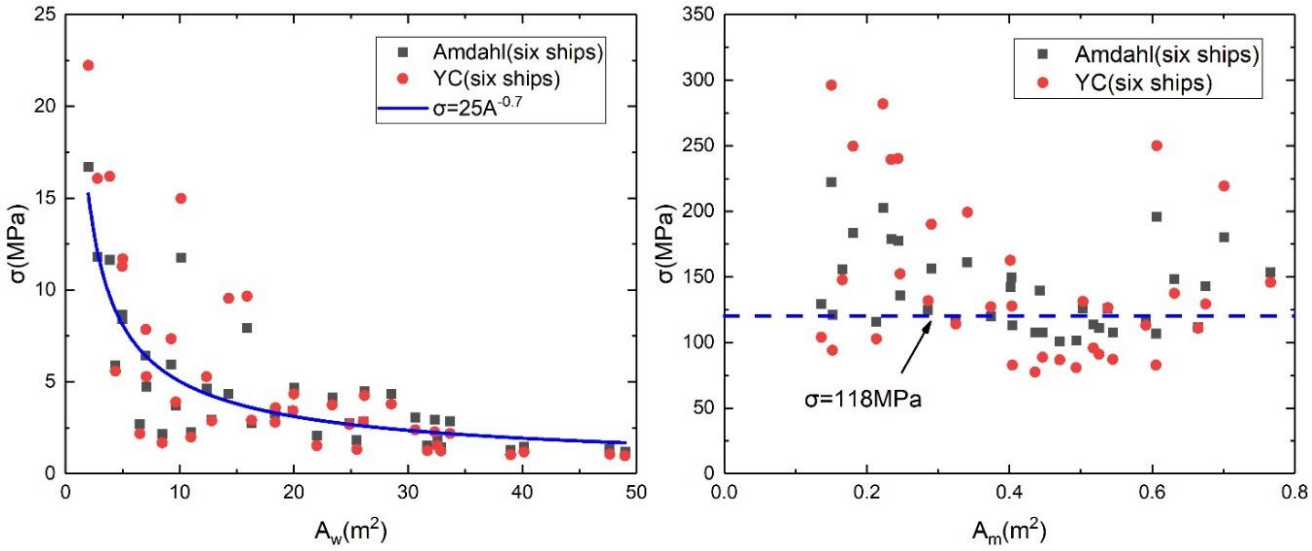

Fig.14. Pressure-area curve for outer bulb cross-sectional area A_w and for material cross-sectional area A_m

The pressure-area curve relation using the outer bulb cross sectional area fitted from Fig.14 is determined as:

$$\sigma_m = 25A_w^{-0.7} \tag{4.19}$$

where $\sigma_m = \frac{F_m}{A_m}$, F_m is the mean crushing force, A_m is the material cross-sectional area, σ_m is the mean crushing stress, A_w is the outer bulb cross-sectional area.

It is seen that expression (4.19) expresses a trend which is similar to formula (4.18) derived for a smaller supply vessel, however, as expected, significantly higher pressures are predicted by Eq. (4.19) for these larger ships.

Also the mean stress 118MPa, which is obtained from formula (4.17), represents the pressure level for most sections of the bow. However, some mean stress values for very small material cross-sectional areas are significantly higher. This is because the tip of the bulbous bow are normally strengthened to protect against accidental impact with anchor chains and floating debris.

5. CONCLUSION

The paper describes an analysis procedure for design of bridge piers against ship collisions such that a given risk acceptance criteria is met.

Firstly, a proposal for elements in risk acceptance criteria is discussed. This is followed by a description of a rational risk assessment procedure. This procedure includes an estimation of the probability for critical meeting situations in the vicinity of the bridge which can cause bridge collisions due to aversive maneuvers, and a procedure for quantitative estimation of the probability for ship collisions. The aim of the probability model is to identify a set of design vessels. A design vessel is here defined as the largest striking ship, a given structural element, such as a bridge pier, must withstand without structural failure in order for the bridge connection to fulfil the risk acceptance criteria.

An important element in such a risk evaluation model is the consequence of collisions between design vessels and bridge piers. Therefore, a detailed analysis is presented of bow impact loads and pressures from six merchant ships of different sizes ranging from 5800DWT to 70000DWT and different speeds against rigid obstacles in the form of piers, or other types of rigid offshore structures. Based on comprehensive numerical calculations, a simple empirical expression is established, Eq. (4.8), which with reasonable accuracy can predict the maximum bow impact force as function of ship impact velocity, ship loading and ship size. This expression allows a rapid prediction method of the maximum collision force. Similar simple expressions is also presented for crushing distances, Eq. (4.10), and for the impact duration, Eq. (4.11). The non-dimensional form of these empirical bow force expressions have been chosen to be similar to those derived in Ref. [15] for ice-strengthened ships. This will facilitate probabilistic analysis involving a mixture of ships with and without ice-class and with different loading conditions.

The newly derived expressions for maximum bow collision forces have been compared with previously published empirical bow crushing forces for ice-strengthened ships [15], with recommendations by IABSE [4] , EUROCODE [5], and with the crushing forces recommended in the US-Guide issued by AASHTO [3]. It is found that the IABSE and the EUROCODE recommended bow forces for ships without ice-strengthening is significantly higher than those resulting from the present analysis. That is, these forces can lead to very conservative designs. The reason for this is that IABSE and EUROCODE recommendations are based on results presented in Ref. [15] which were derived from ships with very high ice class.

On the other hand, the crushing forces recommended by AASHTO significantly underestimates the crushing forces for larger ships. Furthermore, the AASHTO expression is restricted to fully loaded conditions.

Finally, for design of against localized pressure loads on piers and pylons subjected to impacts from the bulb part of the bow, local pressure loads are derived as functions of the outer bulb cross-sectional area Eq. (4.19) as well as the material cross-sectional area.

6. REFERENCES

[1] Moan, T. and Eidem, M. 2019: Floating bridges and submerged tunnels in Norway - The history and future outlook. Proceedings of the World Conference on Floating Solutions Edited by C.M. Wang, S.H. Lim and Z.Y. Tay 22-23 April 2019, Singapore

[2] Pedersen, P. T. 2002: Collision Risk for Fixed Offshore Structures Close to High-density Shipping Lanes. Journal of Engineering for the Maritime Environment, Proceedings of the Institution of Mechanical Engineers, Vol. 216 Part M1 pp. 29 – 44.

[3] AASHTO, 2009: Guide Specification and Commentary for Vessel Collision Design of Highway Bridges. American Association of State Highway and Transportation Officials, Washington DC.

[4] Larsen, O. D. 1993: Ship collision with bridges. Structural engineering document No. 4. . IABSE International Association for Bridge and Structural Engineering.

[5] Eurocode 1 2010: – Actions on Structures – Part 1-7: General actions – Accidental actions. (Incorporated corrigendum February 2010). July 2006 CEN.

[6] Szlapczynski, R. & Szlapczynski, J. 2017: Review of ship domains: Models and applications. Ocean Engineering. Vol 145, pp 277-289.

[7] Fujii,Y. and Mizuki, 1998: Design of VTS Systems for Water with Bridges. Proc. Int. Symposium on Advances in Ship Collision Analysis, Copenhagen Denmark; A.A.Balkema pp. 177-193.

[8] Hansen, M.G.; Jensen, T.K.; Lehn-Schiøler, T.; Melchild, K.; Rasmussen F.M. & Ennemark F. 2013: Empirical Ship Domain based on AIS Data. Journal of Navigation Vol 66, pp. 931-940.

[9] Jensen, T.K.; Hansen, M.G.; Lehn-Schiøler, T.; Melchild, K.; Rasmussen, F.M. & Ennemark, F. 2013: Free Flow Efficiency of a One-way Traffic Lane between two Pylons. Journal of Navigation, 66, 941–951.
[10] Karlson, M., Rasmussen, F. & Frisk, L. 1998. Verification of ship collision frequency model. Proceedings of the International Symposium on Advances in Ship Collision Analysis. Copenhagen Denmark, Editors Gluver & Olsen, Balkema, pp.117–121.
[11] Rasmussen, F.M., Glibbery, K.A.K., Hansen, M.G., Jensen, T.K., Lehn-Schiøler, T. & Randrup-Thomsen, S., 2012: Quantitative assessment of risk to ship traffic in the Fehmarnbelt fixed link project. Journal of Polish Safety and Reliability Association, Summer Safety and Reliability Seminars.Vol.3, No. 1.
[12] Heinrich, H.W. 1959. Industrial Accident Prevention, A Scientific Approach, 4th edition, McGraw Hill, 1959.
[13] Lützen, M. 2001: Ship Collision Damage, PhD thesis, Department of Mechanical Engineering, Technical University of Denmark
[14] Pedersen P.T. & Zhang S., 1998: On Impact Mechanics in Ship Collisions, Journal of Marine Structures, Vol. 11, pp. 429-449.
[15] Pedersen, P. T, Valsgaard,S. Olsen, D. & Spangenberg, S. 1993: Ship Impacts: Bow Collisions. International Journal of Impact Engineering. 13, No. 2: 163-187.
[16] Pedersen, P.T. 2013: Ship collisions against wind turbines, quays and bridge piers. In Proceedings of the 6th International Conference on Collision and Grounding of Ships and Offshore Structures, ICCGS 2013 (pp. 273-280). C R C Press LLC.
[17] Hoang, L. C. & Lützen, M. 2012: Ship collisions with pile-supported structures—estimates of strength and ductility requirements. Structural Engineering International, Vol. 22, No. 3, pp. 359-364(6)
[18] Sha, Y. , Amdahl, J. & Dørum, C. 2017: Dynamic responses of a floating bridge subjected to ship collision load on bridge girders. Procedia Engineering 199, pp. 2506-2513.
[19] Sha YY, and Hao H, 2012. Nonlinear finite element analysis of barge collision with a single bridge pier. Engineering Structures, 41:63-76. https://doi.org/10.1061/10.1016/j.engstruct.2012.03.026
[20] Chen, J.; Zhu, L. and Pedersen, P.T 2019.: On Dynamic effects of Bulbous Bow Crushing, Proceedings of the Twenty-ninth (2019) International Ocean and Polar Engineering Conference, Honolulu, Hawaii, USA, ISBN 978-1 880653 85-2; ISSN 1098-6189
[21] Yamada, Y. & Pedersen, P.T. 2008: A Benchmark Study of Procedures for Analysis of Axial Crushing of Bulbous Bows. Marine Structures. Vol. 21. Issues 2-3, pp. 257 – 293.
[22] Yang, P.D.C. and Caldwell J.B. 1988: Collision Energy Absorption of Ship's Bow Structures". International Journal of Impact Engineering, 7(2): pp. 181-196.
[23] Amdahl J. 1983: Energy Absorption in Ship-platform Impacts. PhD. thesis, Department of Marine Technology, The University of Trondheim. Report No. UR-83-34
[24] Cowper G R, Symonds P. 1957: Strain hardening and strain-rate effects in the impact loading of cantilever beams. Technical Report No. 28, Division of Applied Mathematics, Brown.
[25] Paik J. K. and Thayamballi A. K. 2003: Ultimate Limit State Design of Steel-Plated Structures, Published by John Wiley & Sons Ltd, England.
[26] Minorsky V.U.,1959: An Analysis of Ship Collisions with Reference to Protection of Nuclear Power Ships, J. of Ship Research, Vol. 3, No. 2, pp. 1-4.
[27] Pedersen, P.T., Zhang, S., 2000: Absorbed energy in ship collisions and grounding—revising Minorsky's empirical method. J. Ship Res. 44 (2), 140–154
[28] DNV-RP-204. 2010: Design against accidental loads. Det Norske Veritas, Høvik, Norway.
[29] NORSOK Standard N-400. 2004: Design of steel structures, Appendix A, Design against accidental actions.

[30] Storheim, M. & Amdahl, J. 2014: Design of offshore structures against accidental ship collisions. Marine Structures. Volume 37, pp. 134-172.
[31] Yu, Z & Amdahl, J. 2018: Analysis and design of offshore tubular members against ship impacts. Marine Structures Volume 58, pp. 109-135.

APPENDIX: STRUCTURAL DETAILS OF THE SHIPS UNDER ANALYSIS

5800DWT BULK CARRIER(SEE FIG.A1)

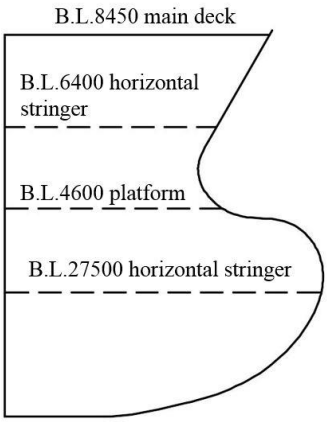

Fig.A1. C.L.PROFILE

The bow is stiffened by transverse stiffeners with spacing 550mm. The yield stress is 316 MPa and ultimate strength is 416 MPa.

B.L.8450 main deck	Plate thickness	8mm
	CL-bulhead	8mm
	C.L.1800 longitudinals	T300X8/100X10
	C.L.3600 longitudinals	T300X8/100X10
	C.L.4800 longitudinals	T300X8/100X10
	CL-girder	Before #150 T300X8/100X10
B.L.6400 horizontal stringer		T670X10/150X12
B.L.4600 platform	Plate thickness	Before #150 7mm After #150 12mm
	CL-girder	Before #150 T350X10/150X12
	C.L.1800 longitudinals	T350X10/150X12
	C.L.3600 longitudinals	T350X10/150X12
B.L.2750 horizontal stringer		T670X10/150X12
Bottom	C.L.1800 side keelson	T10/150X12
Side shell		12mm

12800DWT TANKER (SEE FIG.A2)

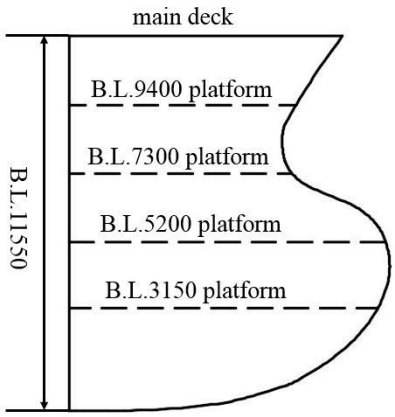

Fig.A2. C.L.PROFILE

The bow is stiffened by transverse stiffeners with spacing 600mm. The yield stress is 316 MPa and ultimate strength is 416 MPa.

Main deck	Plate thickness	10mm
	CL-bulhead	Above B.L.7300platform 9mm Below B.L.7300 platform 12mm
	Deck longitudinals	T450X10/150X12
B.L.9400 platform	Plate thickness	9mm
	Deck longitudinals	T350X8/100X10
B.L.7300 platform	Plate thickness	10mm
	Deck longitudinals	T350X8/100X10
B.L.5200 platform	Plate thickness	9mm
	Deck longitudinals	T350X8/100X10
B.L.3150 platform	Plate thickness	9mm
	Deck longitudinals	T350X8/100X10
Bottom	Center keelson	T12/250X18
	Inner bottom	12mm
Side shell	Below B.L.9400 platform	14mm
	Above B.L.9400 platform	12mm

25000DWT CONTAINER SHIP (SEE FIG.A3)

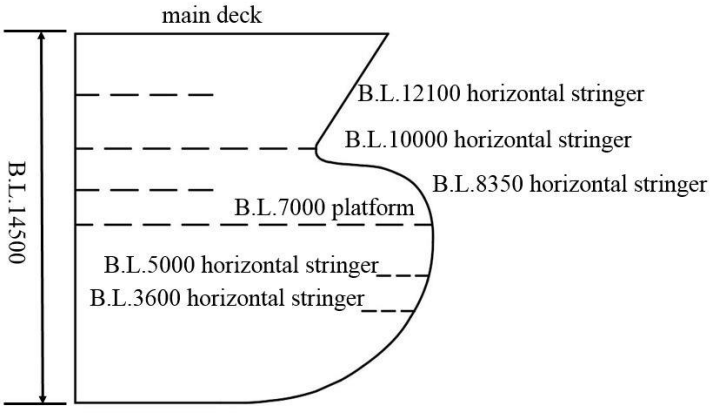

Fig.A3. C.L.PROFILE

The bow is stiffened by transverse stiffeners with spacing 600mm. The yield stress is 316 MPa and ultimate strength is 416 MPa.

Main deck	Plate thickness	10mm
	CL-bulhead	Before #236(between platform and main deck) 12mm
	Deck longitudinals	T400X10/100X12
	CL-girder	T600X12/200X16
B.L.12100 horizontal stringer		T10/150X12
B.L.10000 horizontal stringer	Plate thickness	10mm
C.L.3535 bulkhead		Before #236(between platform and main deck) 12mm
B.L.8350 horizontal stringer	Plate thickness	10mm
B.L.7000 platform	Plate thickness	10mm
	CL-girder	T600X10/150X12
	Deck longitudinals (before #241)	T600X10/100X10
B.L.5000 horizontal stringer		T1000X10/150X12
B.L.3600 horizontal stringer		T1000X10/150X12
Bottom	Center keelson(before #241)	T12/100X12
	Side keelson(before #241)	T12/100X12
Side shell	Plate thickness	14mm

45000DWT BULK CARRIER (SEE FIG.A4)

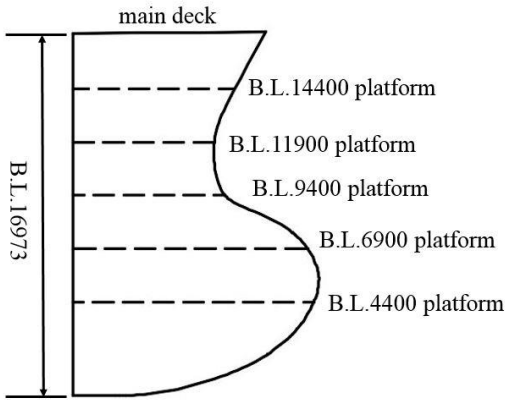

Fig.A4. C.L.PROFILE

The bulbous bow is stiffened by transverse stiffeners with spacing 600mm. The yield stress is 316 MPa and ultimate strength is 416 MPa.

Main deck	Plate thickness	10mm
	Deck longitudinals	HP160X9
	Deck girder	T400X10/200X12
	CL-bulhead	9mm
B.L.14400 platform	Plate thickness	9mm
	Deck girder	T300X9/150X10
B.L.11900 platform	Plate thickness	12mm
	Deck girder	T300X9/100X10

B.L.9400 platform	Plate thickness	12mm
	Deck girder	T300X9/100X10
B.L.6900 platform	Plate thickness	12mm
	Deck girder	T300X9/100X10
B.L.4400 platform	Plate thickness	12mm
	Deck girder	T300X9/100X10
Bottom	Center keelson	T12/250X14
	Side girder	T11/250X12
Side shell	From main deck to 14400 platform	After #209 20mm Before #209 13mm
	From 14400 platform to 11900 platform	After #209 20mm Before #209 16mm
	From 11900 platform to 9400 platform	14mm
	Below 9400 platform	15mm

53500DWT BULK CARRIER (SEE FIG.A5)

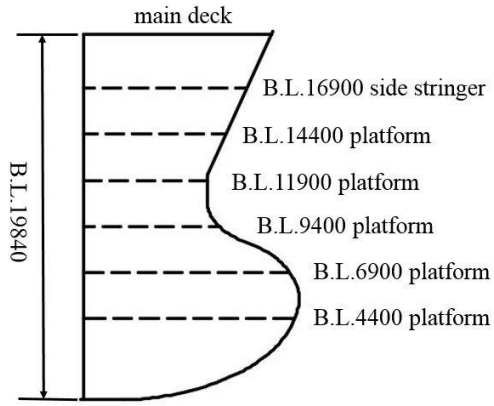

Fig.A5. C.L.PROFILE

The bulbous bow is stiffened by transverse stiffeners with spacing 600mm. The yield stress is 316 MPa and ultimate strength is 416 MPa.

Main deck	Plate thickness	10mm
	Deck longitudinals	HP160X9
	Deck girder	T400X10/200X12
	CL-bulhead	9mm
B.L.16900 side stringer		T600X10/120X12
B.L.14400 platform	Plate thickness	9mm
	Deck girder	T300X9/150X10
B.L.11900 platform	Plate thickness	9mm
	Deck girder	T300X9/150X10
B.L.9400 platform	Plate thickness	12mm
	Deck girder	T300X9/100X10
B.L.6900 platform	Plate thickness	12mm
	Deck girder	T300X9/100X10

B.L.4400 platform	Plate thickness	12mm
	Deck girder	T300X9/100X10
Bottom	Center keelson	T12/250X14
	Side keelson	T11/250X12
	longitudinals	HP280X11
Side shell	From main deck to 16900 side stringer	After #229 13mm From #229 to #225 20mm Before #225 13mm
	From 16900 side stringer to 14400 platform	After #221 16mm Before #221 13mm
	From 14400 platform to 11900 platform	After #221 20mm Before #221 16mm
	From 11900 platform to 9400 platform	14mm
	Below 9400 platform	15mm

70000DWT CONTAINER SHIP (SEE FIG.A6)

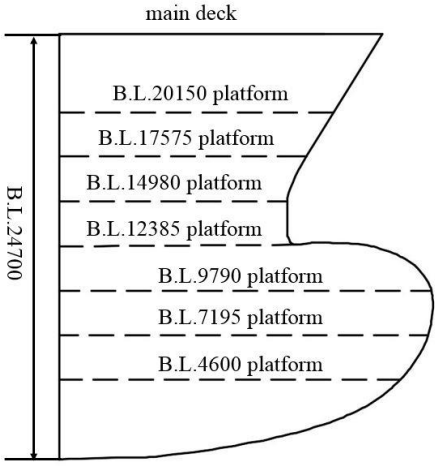

Fig.A6. C.L.PROFILE

The bulbous bow is stiffened longitudinally with spacing 700mm. The yield stress is 426 MPa and ultimate strength is 550 MPa.

Main deck	Plate thickness	12mm
	Deck longitudinals	From #349 to #345 HP200X10 Before #345 HP240X10
	Deck girder	From C.L.4385 T450X10/200X20 C.L. girder T540X10/200X20
B.L.20150 platform	Plate thickness	12mm
	Deck girder	From C.L.2705 T420X9/150X15 C.L. girder T420X11/200X15
	Deck longitudinals	HP200X10
B.L.17575 platform	Plate thickness	12mm
	Deck girder	C.L. girder T400X10/200X15
	Deck longitudinals	HP200X10
B.L.14980 platform	Plate thickness	9mm
	Deck longitudinals	HP180X9
B.L.12385 platform	Plate thickness	12mm
	Deck longitudinals	HP180X9

B.L.9790 platform	Plate thickness	9mm
	Deck longitudinals	HP180X9
B.L.7195 platform	Plate thickness	9mm
	Deck longitudinals	HP200X10
B.L.4600 platform	Plate thickness	9mm
	Deck longitudinals	HP180X9
Inner bottom	Plate thickness	12mm
Longitudinal bulkhead	From main deck to 17575 platform	From #332 to #327 C.L. 15mm
	Below 14980 platform	C.L. 12mm
	From C.L.4270	12mm
	From C.L.7830	12mm
Side shell	Plate thickness	22mm